Melting of transition metals at high pressure and the influence of liquid frustration: The early metals Ta and Mo

Marvin Ross,[1] Daniel Errandonea,[2] and Reinhard Boehler[3]
[1]*Lawrence Livermore National Laboratory, University of California, Livermore, California 94551, USA*
[2]*Departmento de Fisica Aplicada-ICMUV, Universitat de València, Edificio de Investigación, c/Dr. Moliner 50, 46100 Burjassot (Valencia), Spain*
[3]*Max Planck Institut für Chemie, Postfach 3060, D-55020 Mainz, Germany*
(Received 17 July 2007; published 27 November 2007)

In this second report, we focus attention on the role that frustration plays in the melting curves of the early transition metals. Of particular interest are Mo and Ta. This is partly because these metals have nearly half-filled *d* bands implying that a maximum Jahn-Teller distortion is responsible for a high level of liquid frustration leading to melting slopes that are among the lowest observed for transition metals, and partly to resolve an apparent discrepancy between diamond-anvil cell and shockwave-melting measurements. Since the two sets of measurements are nonoverlapping, they are highly complementary, leading to a phase diagram for the two metals that resolves these discrepancies, without challenging the credibility of either set of measurements.

DOI: 10.1103/PhysRevB.76.184118 PACS number(s): 61.25.Mv

I. INTRODUCTION

In the preceding paper,[1] it was shown that the melting temperatures of the late transition metals Ni and Fe are lowered significantly by the presence in the liquid of energetically preferred local structures, or geometric frustration, and attributed to a Peierls–Jahn-Teller (PJT) distortion.[2,3] In contrast to the late transition metals, all the *d* electrons of early transition metals are bonding, allowing for a higher degree of hybridization, stronger directional *d*-orbital bonding, and a stronger PJT distortion. This leads to a higher concentration of preferred local structures and a greater influence on the melting. The melting measurements of the early metals[4,5] are plotted in Fig. 1. The very flat character of the melting curves is notable, and experimentally reproducible.

The PJT distortion is optimal in the case of the metals Mo and Ta, with nearly half-filled bands where the distortion lowers the energy of the occupied bonding states while the unoccupied antibonding states are raised in energy thus forming a narrow band gap. As a result, the measured melting slopes increase sharply for metals that have more than five *d*-valence electrons. This is clearly illustrated by the early and late transition metal melting slopes plotted in Fig. 1 of the preceding paper. In the case of Ta there is experimental[6] and theoretical[7–10] evidence for local structures in liquid and supercooled Ta. These structures have a complex polytetrahedral nature with some icosahedral ordering. Tight-binding band calculations have shown that transition metals with 3–5 *d* electrons favor polytetrahedral structures such as icosahedra and A15.[9,10] While fcc and bcc structures maximize the long range density of closely packed spheres, polytetrahedral structures maximize the short range density of the liquid that favors pressure-induced local frustration.

Mo and Ta are of particular interest here because of the apparent disagreement of diamond-anvil cell (DAC)[4,5,11] and shockwave-melting measurements.[12–14] The original intent of this study was to resolve these discrepancies; however, in the process of examining these measurements we have been led to conclude that both of these sets of experiments are in fact correct. Since the two techniques access very different nonoverlapping regions of the phase diagram, they access different levels of frustration. This leads to phase diagrams that are very unusual for transition metals, and in some respects similar to those of pressure-induced liquid-glass transitions.

The paper is organized as follows. In Sec. II the Mo and Ta shock-melting measurements are examined. In Sec. III, a phase diagram is proposed for Mo and Ta that is consistent with the DAC and shock experiments. In Sec. IV the results of x-ray diffraction experiments made for the detection of melting are presented, along with observational evidence for the presence of local liquid structures. Earlier DAC measurements on Ta and Mo are now strongly supported by the x-ray diffraction measurements. Section V considers the implications of liquid frustration for theoretical modeling, and Sec. VI is a short summary.

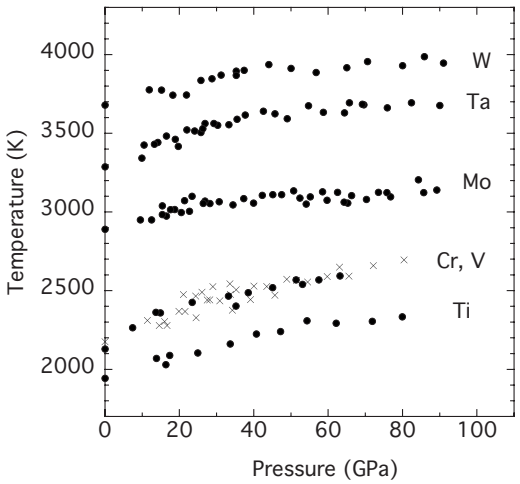

FIG. 1. Melting curve measurements of several early transition metals.

II. Mo AND Ta MELTING

In comparison with the static DAC method, shock or dynamic experiments have access to significantly higher temperatures and pressure. However, the longer time scale and nondestructive nature of DAC experiments allows for accurate temperature measurements and the application of diagnostics unavailable to shock experiments. The techniques employed are well documented. Melting has been detected in the laser DAC method by observing the onset of laser speckle motion in the liquid, changes in optical reflectivity, textural changes, and recently by x-ray diffraction.[1,4,5] In shock experiments melting is determined by detecting discontinuities in the longitudinal sound velocities that occur upon the loss of shear strength in the liquid.[12–14] Since temperature measurements have not proven to be feasible for metals in shock experiments, they need to be calculated. Temperatures depend on estimates of the specific heat and Grüneisen parameter that lead to uncertainties of order ±10%. In addition, diagnostic detection methods suffer from the possibility that the short nanosecond time scales of the shock transit may cause an overshoot of the equilibrium melt pressure resulting in an overestimate of the melting pressure and temperature. In combination, static and dynamic experimental measurements are capable of providing important new insights into the high-pressure and high-temperature phases of frustrated viscous liquids.

A. Mo melting

Plotted in Fig. 2 are the DAC measurements for Mo[4] and Ta,[4,5] their Hugoniot curves,[12,14] and the *P-T* points indicated at which discontinuities have been detected in the longitudinal sound speed. The two sets of experimental data are not overlapping. The DAC measurements for Mo and Ta are roughly in the 3000–4000 K range, and below 100 GPa. The shock measurements are at appreciably higher conditions. For Mo, two transitions are reported at 210 GPa (~4000 K) and at 390 GPa (~9000 K). The first has been interpreted as a bcc-hcp transition and the second as melting to a liquid phase resulting from the loss of shear strength in the shocked solid. However, an extrapolation of the DAC measurements to higher pressure suggests that the 210 GPa shock discontinuity may be melting.

A calculation for a bcc-hcp transition in Mo was reported by Moroni *et al.*[15] They determined the total lattice electronic, thermal electronic, and vibrational contributions of bcc Mo using *ab initio* methods within the framework of the local density theory. They predict a bcc-hcp transition near 8700 K at $P=0$. This is in reasonable agreement with a prediction of 10 000 K near 210 GPa that we[16] obtained in unpublished calculations, employing a method similar to Moroni *et al.* This suggests that this shock transition at 210 GPa is likely due to the onset of melting. Since the second transition near 390 GPa was interpreted as a solid-liquid transition, this raises the question as to the nature of the Mo phase lying between 210 and 390 GPa. We refer to this intermediate state as phase II.

B. Ta melting

In the case of Ta, DAC measurements have detected melting by the laser speckle method.[4] These results have been confirmed by measurements in which melting was also detected by the disappearance of crystalline x-ray diffraction lines.[5] In contrast to Mo, only one transition has been observed in the Ta shock experiments,[14] near 300 GPa (~10 000 K), and it has been interpreted as bcc-liquid melting. This interpretation is inconsistent with an extrapolation of the DAC measurements. But it opens the question to whether there exists a lower pressure shock discontinuity. An inspection of the existing Mo and Ta shock sound speed shock data suggests that the absence of a shock discontinuity in Ta at a lower pressure, analogous to the 200 GPa transition in Mo, is simply due to the absence of sound speed shock measurements.

The longitudinal sound speed shock measurements made for Mo[12] and Ta[14] are plotted in Fig. 3. An inspection of the data shows that for Mo, starting from the normal bcc solid at $P=0$, there is a linear increase in the sound velocity leading to the discontinuity at 210 GPa, and a change in state to

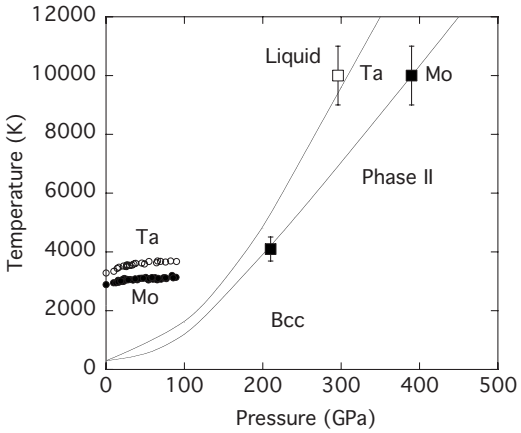

FIG. 2. DAC and shock melting. DAC, Mo (open circles) and Ta (filled circles) (Refs. 9 and 10). Shock, Mo (open squares) (Ref. 12) and Ta (filled squares) (Ref. 14).

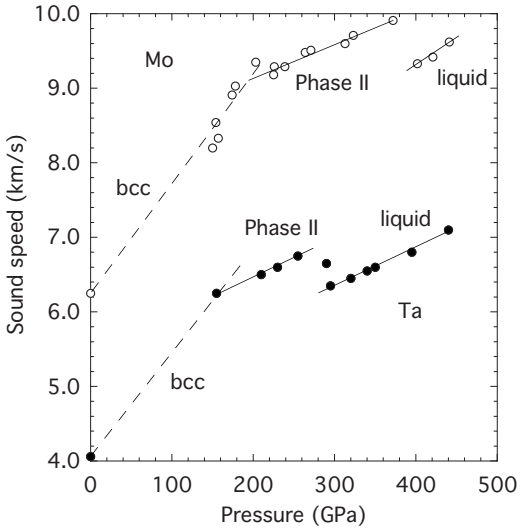

FIG. 3. Sound velocities of Mo (open circles) (Ref. 12) and Ta (filled circles) (Ref. 14) measured along the Hugoniot.

phase II. At 390 GPa there is a sharp discontinuity in the sound speed due to a loss of shear strength to a state with a sound speed equal to that of the liquid bulk sound speed. This transition is interpreted as melting to a liquid. However, in the case of Ta, the lowest sound velocity measurement starts near 150 GPa and increases linearly, but shows only the transition to the liquid near 300 GPa. Absent are any Ta sound speed data below 150 GPa, like those of Mo. However, a dashed line drawn from the 150 GPa data point down to $P=0$ follows the same linear pattern as Mo. This suggests that a bcc to a phase II transition, like that for Mo, should occur in Ta near or below 150–200 GPa. This would place the shock measurements for Ta also in agreement with an extrapolation of the DAC measurements. The situation for shocked V[17] is similar to that for Ta.[18] For V, there is only one transition identified as melting, near 225 GPa (~7800 K), and absent are any sound speed data below 150 GPa. Since the absence of these data is not due to an experimental error, we feel free to assume the existence of a Ta shock discontinuity in the pressure range 150–200 GPa, near 4000 K. This can be validated by carrying out Ta sound speed measurements below 200 GPa.

III. PROPOSED Mo, Ta PHASE DIAGRAM

Despite the extreme physical conditions some insight into the nature of phase II can be extracted from an analysis of the longitudinal sound speeds (C_L). C_L is related to the isothermal bulk modulus (K), and the shear modulus (G) by the expression $C_L=[(K+4/3G)/\rho]^{1/2}$, where ρ is the mass density. In the absence of shear strength, as in the case of an isotropically compressible liquid, $G=0$ and C_L reduces to the bulk sound speed, $C_B=(K/\rho)^{1/2}$. By this method the 390 and 300 GPa discontinuities in Mo and Ta were interpreted as transitions to a liquid phase. Using the bulk sound speed (C_B) obtained from the Hugoniot, and the measured longitudinal speeds (C_L) plotted in Fig. 3, it is possible to extract values of the shear modulus and bulk modulus using the above expressions.

Figure 4 shows a plot of the shear modulus calculated for Mo at each of the experimental shock pressure points. Starting from a value of ~100 GPa there is a flat region, then a steep rise starting at 160 GPa to a maximum at 200 GPa, the pressure at which the sound speed discontinuity from bcc to phase II was detected. With increasing pressure there is a steady decrease in the shear modulus to about 380 GPa, and a sharp drop to $G=0$ GPa in the liquid. The same calculations made for Ta are shown in Fig. 5. Since there were no experimental shock speed measurements made along the Ta Hugoniot below 150 GPa, the values of the shear modulus for bcc Ta were taken from the 0 K calculations of Orlikowski *et al.*[19] The lack of experimental sound speed data for Ta below 150 GPa, and the reliance on 0 K theoretical calculations for the shear modulus, may account for the qualitative difference with Mo.

The crossing of the predicted 0 K bcc shear modulus, and the shear modulus calculated from the shock sound speeds, may be taken as a rough estimate of a Ta bcc to a Phase II transition at 150 GPa. We speculate that phase II has been

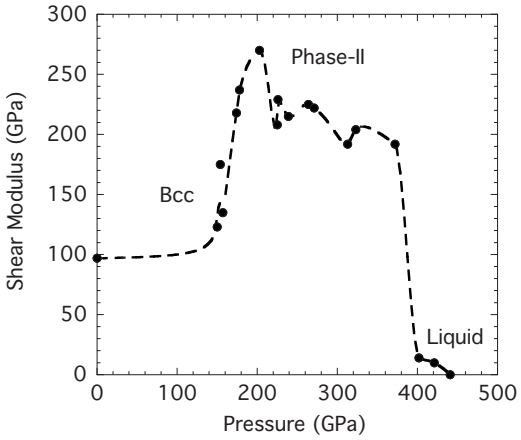

FIG. 4. Shear Modulus (G) calculated for Mo (filled circles) as described in text.

determined by a high concentration of geometrically frustrated preferred structures, and since it supports shear waves it is viscoelastic. Viscous fluids do not support shear waves, but viscoelastic materials do.

A generalized phase diagram in Fig. 6 is proposed for Mo and Ta. At low pressure, the bcc solid melts to a frustrated liquid.[6–10] With increasing pressure the concentration of locally preferred structures increases. The DAC melting measurements, extended linearly, connect to the 210 GPa Mo shock transition and the Ta transition near 150–170 GPa, thereby defining a bcc to a phase II transition boundary. At a very high temperature, near 10 000 K, phase II melts to a normal liquid.

The solid curve is a Ta melting curve calculated by Wang *et al.*[20] employing the Lindemann criterion. A similar curve for Mo has been omitted to avoid visual confusion. Lindemann assumed that a solid melts when the mean-square amplitude of vibration of atoms about their equilibrium position is larger than a fixed fraction of the lattice spacing. The criterion is basically a solid phase scaling model that neglects

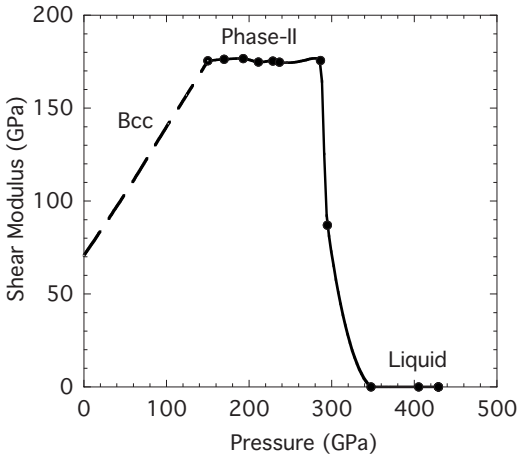

FIG. 5. Shear modulus (G) calculated for Ta (filled circles) as described in text. The values of G below 150 GPa (long-dashed curve) were taken from the calculations at $T=0$ K by Orlikowski *et al.* (Ref. 19).

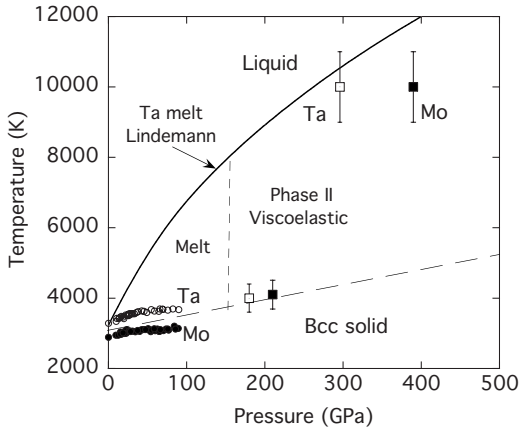

FIG. 6. Proposed phase diagram for Mo and Ta. DAC measurements: Mo (filled square) and Ta (empty square) measurements (Refs. 9 and 10) with linear extrapolation (long dashes). Hugoniots of Mo and Ta with pressures of sound speed discontinuities indicated by filled squares for Mo (Ref. 12). For Ta the data point near 300 GPa was measured (Ref. 14), but near 170 GPa the melting was predicted as described in the text. The Lindemann Ta melting curve is from Wang *et al.* (Ref. 20). Melt-phase II boundary near 150 GPa (short-dashed line).

any influence that changes in the liquid structure might have on the melting. The Lindemann model works well for systems in which the effective interatomic potential remains unchanged on going from solid to liquid.

The Lindemann line defines a hypothetical melting curve for a metal in equilibrium with a "pure" atomic liquid. However, the liquid frustration actually present leads to a lowering of the melting temperature, in which case the Lindemann line may be considered as a rough estimate of the transition zone from a pure liquid, to a frustrated, or supercooled melt. A compression of the melt along a 6000 K isotherm, into phase II, would constitute a supercooled melt to a phase II transition. Recently, Anikeenko and Medvedev,[21] using computer simulations, examined the polytetrahedral nature of dense disordered packings of hard spheres. They determined that the fraction of spheres in polytetrahedral structures increases with compression until all the spheres are in tetrahedra at the Bernal limiting packing fraction of 0.64. In contrast to hard spheres, transition metal tetrahedra are compressible, are stabilized by chemical bonding, and are most likely to remain jammed into a glasslike structure. The vertical dashed line near 150 GPa has been drawn to represent, schematically, the possible existence of such a pressure-induced liquid melt to a glasslike solid transition. This line would constitute the low-pressure boundary of phase II. In the present model, Ta and Mo melt from phase II to a normal liquid, in which case the "Lindemann line" could be redrawn to curve down. However, since the shock-melting temperatures are themselves crude estimates, based on a crystalline solid and a Grüneisen equation of state, this step has been bypassed. Compressing the melt into phase II can be considered as analogous to the temperature lowering of a supercooled liquid into a glass.

IV. DIAMOND-CELL X-RAY DIFFRACTION EXPERIMENTS AND THE DETECTION OF Mo MELTING

While the proposed phase diagram is consistent with the currently available set of experimental high-pressure data, its validation requires additional experimental study. In earlier experiments, made in a laser heated DAC for Ti, Ta, and W, at pressures up to 100 GPa,[4] melting was observed by the appearance of fluidlike material motion in the sample hot spot and by the observation of typical melt features on the surface of the quenched samples. These measurements were confirmed in a separate set of experiments where Ta melting was also detected, but by x-ray diffraction methods using double-sided laser heating[5] and taking diffraction patterns in steps of 50 K. Temperature was measured *in situ* from both sides of the sample.

Recently we made similar x-ray diffraction experiments for Mo at 55 GPa at the ID27 beamline of the European Synchrotron Radiation Facility (ESRF) using the setup described in Schultz *et al.*[22] and combined with a fast data collection. These measurements provided two important facts. First, as the temperature was raised, the grain size of the polycrystalline sample grew, and the diffraction pattern changed from continuous (Debye-Scherer) rings to a spotty pattern as the x-ray beam encountered fewer, but larger, crystals. Second, upon further increasing the temperature to near the melting point of 3200 ± 100 K, rapid recrystallization and grain growth was observed and subsequently, at 3300 ± 100 K, the spotty pattern degenerated into a diffuse ring of scattering, which we attributed to the fact that the studied sample was fully melted in agreement with earlier work.[4] The difference between the patterns produced by the solid and the liquid was clear and unmistakable.

Basically, we found that the x-ray diffraction experiments are in good agreement with our DAC measurements. At low pressures ($P < 40$ GPa) the Mo melting temperature determined using x-ray diffraction agrees within the experimental uncertainties with the melting temperature visually determined from the movement of the laser speckle on the hot spot. At the highest pressure (~ 100 GPa) the maximum difference is about 150 K. This difference is likely due to the increasing temperature gradient in the sample at higher pressures and the fact that in the x-ray diffraction experiments melting is determined from the bulk, while in the optical experiments melting is determined from the surface. In the x-ray diffraction experiments, as the samples cooled down below the melting point, the diffraction spots reappeared at the same time that the diffuse ring disappeared, indicating that the diffraction pattern changes were not related to any chemical decomposition of the sample.

Some observations are interesting to note since they may provide useful insight into the nature of the melt. When the melting temperature was reached, the laser power heating the sample was kept constant and we kept acquiring diffraction patterns. The sample showed permanent, rapid recrystallization, with a dramatic change of the Bragg peak intensity, from one solidlike diffraction pattern to the next, probably

due to locally preferred orientation nucleation during recrystallization. We attribute this to a continuous change from a solid to a liquid, with a small, difficult to detect, melt fraction. This observation is consistent with a very low melting slope, and a ΔV close to zero, in accordance with the Clapeyron equation. In terms of dynamics, this recrystallization at the melting temperature differs entirely from that observed below the melting temperature and we conclude that it must involve the liquid state. The fact that this liquid is not detectable by x rays is likely due to the presence of clusters.

Continuous melting and nucleation are known to cause textural changes, or turbidity, typically evidence for the presence of inelastic light scattering by impurities in a liquid, or in the present case by bcc or icosahedral short-range order (ISRO) clusterlike materials. If ISROs are present in liquid Ta and Mo, as indeed it is in two other bcc melting metals Ti (Refs. 23 and 24) and Zr,[24,25] then it is quite possible that the phenomena we observed are due to a nucleation of ISRO clusters in the melt at the interface of the Ta sample and the pressure medium. At this point, however, we cannot state with confidence that we observed ISRO clusters floating in the melt, since such measurements are not yet feasible. Additional research is planned. However, the conclusions reached so far should also be applicable to neighboring early transition metals.

V. THEORETICAL CONSIDERATIONS

For the past several years there has been a continuous flow of new experimental and theoretical evidence arguing for the presence of polytetrahedral structures in transition metal liquids.[6–10,22–24] As a consequence, rigorous calculations for the properties of transition metal liquids must account for their influence. At the most elementary level liquid structures are impurities that lower the freezing point. There have been several calculations of the Mo melting curve. The most recent of these, by Cazorla *et al.*,[26] is plotted in Fig. 7, and is clearly in disagreement with the melting measurements plotted in Fig. 1. The results of several other calculations,[31,32] not shown, are in similar disagreement with the experimental DAC measurements.

The reason for the failure of the theoretical methods comes down to the fact that they all neglect the presence of local structures in the liquid. For example, Cazorla *et al.* employed the same embedded atom model (EAM) potential for the liquid and for the solid. As a consequence, since the EAM potential function does not include the directed bonding needed to simulate the polytetrahedral structures any influence of frustration is necessarily omitted from their liquid calculations. A true *ab initio* or *first-principles* calculation would include Jahn-Teller distortions. A phenomenological approach, such as an EAM potential, requires modeling in these effects. By explicitly neglecting *d*-band effects the EAM potential treats Mo as a polyvalent metal. This can be shown simply by noting the agreement, in Fig. 7, of the calculated Mo melting curve with the DAC and shock-melting measurements for Al and Cu.

Cazorla *et al.* have concluded, on the basis of their EAM calculations, that the anomalously low dT/dP of melting is not a consequence of pressure-induced *d*-electron effects, as had been suggested by Ross *et al.*[11] While *d*-electron effects will occur in the solid and the liquid, they do not cancel because preferred structures form in the liquid and are absent in the crystalline solid.[11] If local distortions were present in the solid, there would occur a transformation in the crystal structure. However, bcc is known to be the stable Mo phase at room temperature to a pressure of at least 416 GPa.[33] Another alternative for a solid suffering from distortion is to melt. That appears to be the path chosen by Mo.

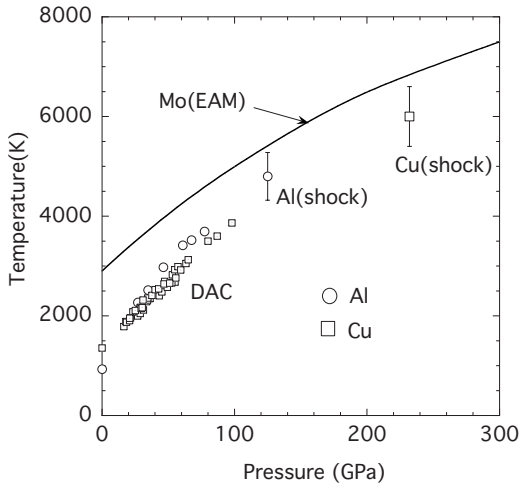

FIG. 7. Mo melting curve calculated by the EAM method (Ref. 26) compared with DAC Cu (open circles) (Ref. 27) and Al (filled circles) (Ref. 28) and shock-melting measurements as labeled (Refs. 29 and 30).

At the completion of this study a paper on Ta melting appeared by the same authors[34] as the Mo paper,[26] employing the same method, and not surprisingly coming to the same conclusions. Our response to their Ta melting paper is equally redundant. Their Ta EAM calculations fail to account for the presence in the liquid of preferred structures. In fact it is easily shown that their Ta melting curve falls on the Ta Lindemann melting curve plotted in Fig. 6. This is a consistent result, since both models neglect local liquid structure.

Luo and Swift[35,36] have recently reported an analysis of the high-pressure melting data of Ta and Mo. They concluded that the failure of theoretical methods to reproduce the DAC melting curve undermines their predictive capability, and that the melting points inferred from shockwave experiments cannot be reconciled by superheating. We agree with their assessment.

VI. SUMMARY

In the present and preceding papers, we have attempted to show that frustration due to preferred structures with local *d*-electron bonding can play an important role in determining the phase diagram of transition metal liquids. The phase diagram for Mo and Ta proposed here has the virtue that it removes the apparent discrepancies existing between shock-wave and diamond-anvil cell experiments without challenging the credibility of either set of measurements. While there

is a considerable amount remaining to be understood, the phase diagram is consistent with our understanding of the physical origin and behavior of frustrated liquids. In combination, the two very different experimental techniques, static and dynamic, exploring a wide range of different conditions, provide valuable insights into the theory of frustrated liquids over an unusually large range of pressure and temperature. A complete theory of transition metal melting will need to include *s-d* transfer, Jahn-Teller distortions, and jamming of local structures. Absent such a computational effort we have chosen to critique the available experiments and calculations in terms of well established principles of chemical physics and electronic structure.

ACKNOWLEDGMENTS

The work by M.R. was partially supported under the auspices of the U.S. Department of Energy by the University of California Lawrence Livermore National Laboratory under Contract No. W-7405-ENG-48. D.E. acknowledges the financial support of the Spanish McyT through the RyC program. M.R. and D.E. also wish to thank the Max-Planck-Institut für Chemie at Mainz, Germany for its hospitality and the Alexander von Humboldt Foundation for its generous support.

[1] M. Ross, R. Boehler, and D. Errandonea, preceding paper, Phys. Rev. B **76**, 184117 (2007).
[2] H. A. Jahn and E. Teller, Proc. R. Soc. London, Ser. A **161**, 220 (1937).
[3] J. K. Burdett, *Chemical Bonding in Solids* (Oxford University Press, Oxford, 1995).
[4] D. Errandonea, B. Schwager, R. Ditz, R. Boehler, and M. Ross, Phys. Rev. B **63**, 132104 (2001).
[5] D. Errandonea, M. Somayazulu, D. Häusermann, and D. Mao, J. Phys.: Condens. Matter **15**, 7635 (2003); D. Errandonea, Physica B **357**, 356 (2005).
[6] L. Cortella, B. Vinet, P. J. Desré, A. Pasturel, A. T. Paxton, and M. van Schilfgaarde, Phys. Rev. Lett. **70**, 1469 (1993).
[7] C. Berne, A. Pasturel, M. Sluiter, and B. Vinet, Phys. Rev. Lett. **83**, 1621 (1999).
[8] N. Jakse and A. Pasturel, J. Chem. Phys. **120**, 6124 (2004).
[9] P. Turchi, G. Treglia, and F. Ducastelle, J. Phys. F: Met. Phys. **13**, 2543 (1983).
[10] R. Phillips and A. E. Carlsson, Phys. Rev. B **42**, 3345 (1990).
[11] M. Ross, L. H. Yang, and R. Boehler, Phys. Rev. B **70**, 184112 (2004).
[12] R. S. Hixson, D. A. Boness, J. W. Shaner, and J. A. Moriarty, Phys. Rev. Lett. **62**, 637 (1989).
[13] J. A. Moriarty, Phys. Rev. B **45**, 2004 (1992).
[14] J. M. Brown and J. W. Shaner, *Shock Waves in Condensed Matter*, edited by J. R. Asay, R. A. Graham, and G. K. Straub (Elsevier Science, New York, 1983).
[15] E. G. Moroni, G. Grimvall, and T. Jarlborg, Phys. Rev. Lett. **76**, 2758 (1996).
[16] M. Ross (unpublished).
[17] C. Dai, X. Jin, X. Zhou, J. Liu, and J. Hu, J. Phys. D **34**, 3064 (2002).
[18] M. Ross, R. Boehler, and S. Japel, J. Phys. Chem. Solids **67**, 2178 (2006).
[19] D. Orlikowski, P. Söderlind, and J. Moriarty, Phys. Rev. B **74**, 054109 (2006).
[20] Y. Wang, R. Ahuja, and B. Johansson, Phys. Rev. B **65**, 014104 (2001).
[21] A. V. Anikeenko and N. N. Medvedev, Phys. Rev. Lett. **98**, 235504 (2007).
[22] E. Schultz, M. Mezouar, W. Critchton, S. Bauchau, G. Blattmann, D. Andrault, G. Fiquet, R. Boehler, N. Rambert, B. Sitaud, and P. Loubeyre, High Press. Res. **25**, 71 (2005).
[23] G. W. Lee, A. K. Gangopadhyay, K. F. Kelton, R. W. Hyers, T. J. Rathz, J. R. Rogers, and D. S. Robinson, Phys. Rev. Lett. **93**, 037802 (2004).
[24] T. H. Kim and K. F. Kelton, J. Chem. Phys. **126**, 054513 (2007).
[25] T. Schenk, D. Holland-Moritz, V. Simonet, R. Bellissent, and D. M. Herlach, Phys. Rev. Lett. **89**, 075507 (2002).
[26] C. Cazorla, M. J. Gillan, S. Taioli, and D. Alfè, J. Chem. Phys. **126**, 194502 (2007).
[27] S. Japel, R. Boehler, B. Schwager, and M. Ross, Phys. Rev. Lett. **95**, 167801 (2005).
[28] R. Boehler and M. Ross, Earth Planet. Sci. Lett. **153**, 227 (1997).
[29] J. W. Shaner, J. M. Brown, and R. G. McQueen, in *High Pressure in Science and Technology*, edited by C. Homan, R. K. MacCrone, and E. Whalley (North Holland, Amsterdam, 1984), pp. 137–141.
[30] D. Hayes, R. S. Hixson, and R. G. McQueen, in *Shock Compression of Condensed Matter 1999*, edited by M. D. Furnish, L. C. Chhabildis, and R. S. Hixson (American Institute of Physics, Melville, NY, 2000), p. 483.
[31] A. B. Belonoshko, S. I. Simak, A. E. Kochetov, B. Johansson, L. Burakovsky, and D. L. Preston, Phys. Rev. Lett. **92**, 195701 (2004).
[32] A. K. Verma, R. S. Rao, and B. K. Godwal, J. Phys.: Condens. Matter **16**, 4799 (2004).
[33] A. L. Ruoff, H. Xia, H. Luo, and Y. K. Vohra, Rev. Sci. Instrum. **61**, 3830 (1990).
[34] S. Taioli, C. Cazorla, M. J. Gillan, and D. Alfè, Phys. Rev. B **75**, 214103 (2007).
[35] S. N. Luo and D. C. Swift, Physica B **388**, 139 (2007).
[36] S. L. Webb, in *Mineral Behavior at Extreme Conditions/EMU Notes in Mineralogy*, edited by R. Miletich (Etövös University Press, Budapest, 2005), Vol. 7, pp. 65–94.